

## A Finite Element Analysis of an Osteoarthritis Knee Brace

D. Stamenović<sup>1,\*</sup>, M. Kojić<sup>2,3,4</sup>, B. Stojanović<sup>5</sup>, D. Hunter<sup>6</sup>

<sup>1</sup> Department of Biomedical Engineering, Boston University  
Boston, Massachusetts, USA

<sup>2</sup> Harvard School of Public Health, Boston, Massachusetts, USA

<sup>3</sup> Research and Development Center for Bioengineering BIOIRC, Kragujevac, Serbia

<sup>4</sup> Department of Biomedical Engineering, The University of Texas Health Science Center at  
Houston, Houston, Texas, USA

<sup>5</sup> Faculty of Natural Sciences and Mathematics, University of Kragujevac, Kragujevac, Serbia

<sup>6</sup> New England Baptist Hospital and Boston University School of Medicine,  
Boston, Massachusetts, USA

dimitrij@bu.edu

*\*Corresponding author*

### Abstract

Knee osteoarthritis is a chronic disease that requires a long term therapeutic intervention. Symptoms of osteoarthritis are associated with altered load distributions across the knee caused by knee malalignment, which promotes disease progression. Biomechanical studies have demonstrated that the varus malalignment of the knee can be corrected with application of a knee brace. Although knee braces have shown to be both efficacious and safe in correcting the malalignment, their current designs are not commonly prescribed due to their bulkiness which creates discomfort and difficulties to patients during prolonged periods of application. Here we propose a novel design of a light, inflatable (pneumatic) knee brace which is made of soft conforming materials. Using a finite element analysis, we show that with a moderate level of inflating pressure this pneumatic knee brace can produce an unloading abduction moment that could completely attenuate the negative effect of the external adduction moment in a fully extended varus knee and thus alter the rate of disease progression.

**Key words:** osteoarthritis, adduction moment, pneumatic knee brace, pressure, finite element analysis

### 1. Introduction

Knee osteoarthritis (OA) is the most common joint disease that affects ~30% of adults over 55 years of age, two thirds of whom are women (MMWR, 1998; Lawrence et al., 1998). It is associated with deterioration of all of the tissues of the synovial joint organ in the knee which can be caused by various factors including injury, genetics, repetitive strain on the knee, obesity, etc. In the absence of a cure for the disease, current therapies are primarily aimed at reducing pain and improving joint function by drugs which are associated with high rates of adverse events (Felson et al., 2000; Jones, 2002; Juni et al., 2002). In addition, these drugs

rarely relieve symptoms completely (Todd and Clissold, 1990). Many individuals with knee OA will ultimately require total knee replacement, a procedure that is also not without inherent morbidity and cost (Zhang et al., 2008). Thus, there is the need to develop alternative, efficacious, non-pharmacologic and non-surgical treatments that are capable of ameliorating the symptoms of OA.

Symptoms of OA are associated with altered load distributions across the knee, which cause an increase in the contact pressure on the tibiofemoral joints thereby promoting disease progression. The most influential factor affecting load distributions across the knee is malalignment. Any shift from the collinear alignment, where the loading axis passes through the hip, knee and ankle (Fig. 1 right), affects load distribution at the knee. In a varus deformed knee (Fig. 1 left), this axis passes medially from the knee center, resulting in an excessive adduction moment at the knee which leads to an increase in contact pressure on medial tibiofemoral joint cartilage. Varus malalignment has been shown to increase OA progression in 70% persons with knee OA (Sharma et al., 2001).



**Fig. 1.** Any shift from the collinear alignment where the loading axis (red line) passes through the hip, knee and ankle (*right*) affects load distribution at the knee. In a varus deformed knee (*left*), this axis passes medially from the knee center, resulting in excessive adduction moments at the knee which leads to an increase in contact pressure (blue arrows) on the tibiofemoral joints.

Knee braces have been used to correct varus malalignment (Komistek et al., 1999). The brace provides a three-point leverage system of forces which creates an abduction moment that counterbalances the excessive adduction moment and thus reduces the contact pressure exerted on the knee in the medial compartment (Fig. 2). Clinical studies have shown that knee braces reduce this pressure by nearly 11% (Lindenfeld et al., 1997; Pollo et al., 2002), as well as the level of pain associated with it by up to ~50% (Kirkley et al., 1999). Despite these positive effects, knee OA braces are not widely used. The primary reasons for this are their bulkiness, style and application (Giori et al., 2004). Existing knee OA braces use technology and materials for cruciate deficient knees (typically young athletes). They consist of a frame made of hard materials (e.g., metal, plastics), hinged at the knee and fastened to the leg by straps that

are often too bulky for older adults (predominantly women) to wear comfortably for long periods. Thus, there is a need to overcome these fundamental limitations of the current knee OA brace design whilst maintaining the clinical efficacy.

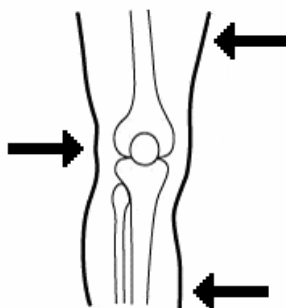


**Fig. 2.** A schematic depiction of the front view of the leg with a three-point-bending system of forces (arrows) applied by a brace to the knee. One of the forces acts at the lateral side and two at the medial side of the knee.

Our ultimate goal is to develop a lightweight knee OA brace using a pneumatic (i.e., inflatable) three-point force leverage and soft conforming materials for a brace that would overcome the fundamental limitations of existing brace designs, whilst still being effective at unloading the affected compartment of the knee. In this study, we propose a novel design of a pneumatic knee OA brace and analyze its performance in the case of a fully extended knee using a finite element analysis. We show that with a moderate level of inflating pressure, this design can unload a greater fraction of the excessive adduction moment than currently existing braces.

## 2. Modeling and analysis

A governing principle that we use in our brace design is based on the following observations (Schipplein et al., 1991; Hurwitz et al., 2002):

The mean maximum magnitude of the adduction moment during normal gait is  $\sim 3.3\%$  of body weight ( $W$ ) times height ( $h$ ).

In patients with medial OA this moment increases to  $\sim 4.2\%W \times h$ .

Thus, our goal is to design a brace that can attenuate the excessive adduction moment ( $\Delta M$ ) which is approximately

$$\Delta M \approx 1\%W \times h \quad (1)$$

The model consists of three major components: a sock, three bladders and a strap (Fig. 3). There are anterior and posterior circular openings in the sock (holes) in order to facilitate easy flexing of the knee. The role of the sock (made of soft elastic material such as neoprene) is to apply the brace around the knee and hold it there via elastic forces of the sock material. The latex bladders are located at the three strategic points around the knee in order to create the three-point leverage system (see Fig. 2). The bladders are firmly attached to the inner side of the strap, and sandwiched between the neoprene sock and the strap, which goes around the knee

(Fig. 3). The strap is made of a light but sturdy nylon fabric. When the bladders are inflated, they push against the leg and the strap. As a result, the strap becomes stressed. Together, stress in the strap and pressure in the bladders produce the three force leverage system which creates an abduction moment. It is assumed that all bladders are inflated to the same pressure. Since the bladders are an integral part of the strap, and since the elastic modulus of the latex bladders is much smaller than that of the nylon fabric strap ( $\sim 10^0$  MPa vs.  $\sim 10^3$  MPa) (cf. Ashby et al., 2007), we assume that the parts of the strap where the bladders are located have approximately the same mechanical properties as the rest of the strap. In order to calculate the abduction moment as well as distributions of stresses and strains within the brace at various levels of inflating pressure, we use a finite element analysis.

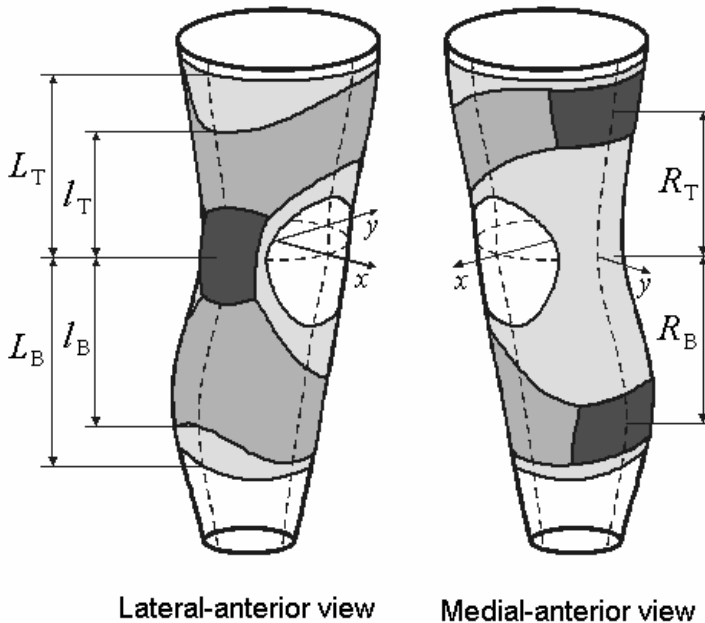


**Fig. 3.** The basic design of the pneumatic knee brace which is comprised of a sock (light gray), a strap (medium gray) and three bladders (dark gray) attached to the strap. By inflating the bladders, a three-point-leverage system of forces is generated.

### 2.1 Finite-element analysis

The leg-brace assemblage in Fig. 3 is considered as a single mechanical system, where brace materials and knee tissue have properties of linearly elastic (Hookean) solids. However, displacement gradients of the brace components due to inflation of the bladders are large and thus the whole assemblage represents a non-linear mechanical system. Equilibrium configurations of the leg-brace assemblage when subjected to pressure loading due to bladder inflation can be calculated in an incremental-iterative scheme using a finite element analysis as described below.

The inflating pressure of the bladders is increased incrementally. At equilibrium configurations, following discrete loading steps, finite-element nodal forces generated by the stresses within the deformed material must balance external loading (i.e., pressure) of the structure. An incremental-iterative equilibrium equation for a finite element can be written as follows (Kojić et al., 2008)

$$\left( {}^{n+1}\mathbf{K}_L + {}^{n+1}\mathbf{K}_{NL} \right)^{(i-1)} \Delta \mathbf{U}^{(i)} = {}^{n+1}\mathbf{F}^{ext} - {}^{n+1}\mathbf{F}_{int}^{(i-1)} \quad (2)$$

where  ${}^{n+1}\mathbf{K}_L$  and  ${}^{n+1}\mathbf{K}_{NL}$  are linear and nonlinear element stiffness matrices, respectively,  $\Delta \mathbf{U}^{(i)}$  is the incremental nodal displacements vector and  ${}^{n+1}\mathbf{F}^{ext}$  and  ${}^{n+1}\mathbf{F}_{int}^{(i-1)}$  are the external and internal nodal forces, respectively; superscript  $n+1$  denotes the end of a load step ( $n$  = step number) and superscript  $i$  is the iteration counter for the equilibrium iterations within the current time step. Iterations are terminated when the unbalanced forces on the right-hand side of Eq. (2), for the assemblage of the finite elements, is small enough (within a numerical tolerance).

In general, the stiffness matrices can be expressed as follows

$${}^{n+1}\mathbf{K}_L = \int_{{}^{n+1}V} {}^{n+1}\mathbf{B}_L^T {}^{n+1}\mathbf{C} {}^{n+1}\mathbf{B}_L dV \quad \text{and} \quad {}^{n+1}\mathbf{K}_{NL} = \int_{{}^{n+1}V} {}^{n+1}\mathbf{B}_{NL}^T {}^{n+1}\hat{\boldsymbol{\sigma}} {}^{n+1}\mathbf{B}_{NL} dV \quad (3)$$

where  ${}^{n+1}\mathbf{B}_L$  and  ${}^{n+1}\mathbf{B}_{NL}$  are the linear and the non-linear strain-displacement matrices, respectively,  ${}^{n+1}\mathbf{C}$  is the constitutive matrix representing the stress-strain relationship,  ${}^{n+1}\hat{\boldsymbol{\sigma}}$  is the stress matrix, and  ${}^{n+1}V$  is the volume of the finite element. These matrices change over iterations.

The internal force vector can be expressed as follows

$${}^{n+1}\mathbf{F}_{int}^{(i-1)} = \int_{{}^{n+1}V^{(i-1)}} {}^{n+1}\mathbf{B}^{(i-1)T} {}^{n+1}\boldsymbol{\sigma}^{(i-1)} dV \quad (4)$$

where  ${}^{n+1}\boldsymbol{\sigma}^{(i-1)}$  is the vector of Cauchy stresses corresponding to strains  ${}^{n+1}\mathbf{e}^{(i-1)}$  at a material point.

The constitutive matrix is calculated as follows

$${}^{n+1}\mathbf{C}^{(i-1)} = \frac{\partial {}^{n+1}\boldsymbol{\sigma}^{(i-1)}}{\partial {}^{n+1}\mathbf{e}^{(i-1)}} \quad (5)$$

Since we assume linearly elastic materials, the constitutive matrix is represented by the elastic matrix  $\mathbf{C}^E$  for each material component of the brace.

Using specially developed software (pre- and post-processors for the solver PAK) (Kojić et al., 1998), the finite-element model of the OA brace is parametrically generated. All three parts of the brace (sock, strap and bladders) are modeled using 4-node shell elements with linear material characteristics (Fig. 4).

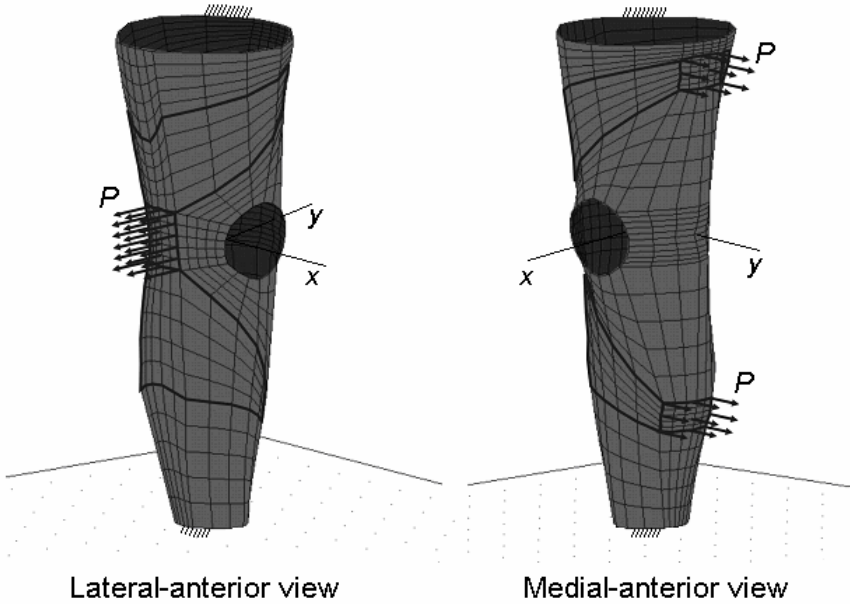


**Fig. 4.** Lateral-anterior view (left) and medial-anterior view (right) of the finite-element model of leg-brace assemblage totally constrained at top and bottom. Lateral and medial bladders are inflated by pressure ( $P$ ). Heavy black lines indicate contours of the strap and the bladders.

The boundary conditions for the computational model are as follows. It is assumed that the top and the bottom end of the brace do not move relative to the leg in order to maintain stability of the leg-brace system. Since the sock material is relatively soft in comparison with the other components of the assembly, these constraints do not affect overall brace stiffness and the mechanical response of the model. The contact between the leg and the brace is modeled using fictive trusses normal to the leg at all shell nodes. The boundary at the brace-leg interface is assumed to be rigid in order to prevent the brace to move perpendicularly toward the leg. The brace is allowed to slide relative to the leg surface and the interface between the brace and the leg is assumed to be frictionless. The mechanical action of the pressure within the bladder on the brace is modeled by applying distributed uniform surface loading to the inner wall of shell elements (Fig. 4).

A nonlinear finite-element analysis is performed using the PAK finite-element solver (Kojić et al., 1998). Forces acting on the leg are calculated as a part of the result post-processing. These forces are separated into two groups: forces from inflating pressure ( $P$ ) of the bladders, and contact forces between the brace and the leg. The net pressure force  $\mathbf{F}_p$  at one bladder is obtained as follows

$$\mathbf{F}_p = P \sum_e \int_{A^e} \mathbf{n} dA = P \sum_e \sum_K \int_{A^e} N_K^e \mathbf{n} dA = \sum_K \mathbf{F}_p^K \quad (6)$$

where  $\mathbf{n}$  is the normal vector to the shell surface,  $N_K^e$  and  $A^e$  are the interpolation functions and the surface area for the  $e$ -th element, respectively; and  $\mathbf{F}_p^K$  is the shell nodal force at the  $K$ -th node due to  $P$ ; the summations over  $e$  and  $K$  are performed over all shell elements and shell nodes of the bladder, respectively. The contact forces represent the forces in the fictitious

trusses ( $\mathbf{F}_C^J$  for the  $J$ -th truss). The pressure and contact forces are evaluated for each loading step.

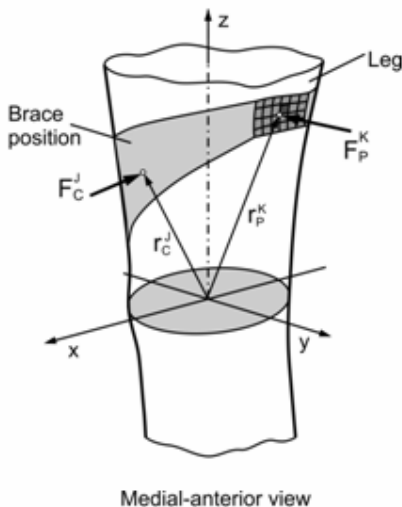


**Fig. 5.** The abduction moment is calculated as a cross product between the radius vectors ( $\mathbf{r}_P^K$  and  $\mathbf{r}_C^J$ ) and corresponding forces acting on the leg [Eq. (7)], including the proximal medial bladder nodal force  $\mathbf{F}_P^K$ , calculated as the sum of the surface integrals of pressure  $P$  over the bladder area [Eq. (6)], and the brace-leg contact forces  $\mathbf{F}_C^J$ , calculated at all contact nodes as forces in fictive trusses.

The abduction moment ( $M$ ) due to action of the brace on the leg is determined by calculating moments of all forces from one side of the mid  $xy$ -plane of the knee, with respect to the  $x$ -axis (Fig. 5)

$$M = \sum_K (y_K F_{Pz}^K - z_K F_{Py}^K) + \sum_J (y_J F_{Cz}^J - z_J F_{Cy}^J) \tag{7}$$

where  $y_K$  and  $z_K$  are the coordinates of shell nodal points of the bladder finite-element model, and  $F_{Py}^K$  and  $F_{Pz}^K$  are components of the pressure nodal force  $\mathbf{F}_P^K$ ;  $y_J$  and  $z_J$  are coordinates of the point of action of the contact force  $\mathbf{F}_C^J$  (with components  $F_{Cy}^J$  and  $F_{Cz}^J$ ); the position vectors of points where the forces  $\mathbf{F}_P^K$  and  $\mathbf{F}_C^J$  are acting are  $\mathbf{r}_P^K$  and  $\mathbf{r}_C^J$ , respectively (see Fig. 5). The first sum includes all nodal points of the bladder model and the second sum is over trusses, in the domain  $z > 0$ .

Distributions of displacements, effective strain and effective (von Mises) stress in the brace components, of pressure exerted by the brace on the knee and the unloading abduction moment  $M$  are calculated for different levels of  $P$ , ranging from 0 to 48 kPa, in ten equal increments of 4.8 kPa. This range of  $P$  is chosen considering that pressures applied by the brace on the leg should not have a negative effect on the blood circulation through the leg nor they should produce pain and discomfort. Values of geometrical parameters (see Fig. 3) are assigned based

on the leg anatomy as follows:  $L_B = 25$  or  $30$  cm,  $L_T = 20$  cm,  $l_T = 10$  or  $15$  cm,  $l_B = 15$  or  $20$  cm,  $R_T = 13$  or  $16.5$  cm,  $R_B = 15$  or  $18.5$  cm. The sizes of the bladders, the medial bladders  $6 \times 3$  or  $6 \times 6$  cm and the lateral bladder  $6 \times 6$  cm, are selected such that when pressurized, the bladders could apply force on the leg that would create a sufficient  $M$  that can attenuate an excessive adduction moment. The size of the hole diameter is  $8$  cm. Elastic modulus and Poisson's ratio of the strap  $E_{\text{strap}} = 3000$  or  $5000$  MPa and  $\nu_{\text{strap}} = 0.3$ , respectively and of the sock  $E_{\text{sock}} = 1$  or  $3$  MPa and  $\nu_{\text{sock}} = 0.43$  reflect material properties of nylon fabric and neoprene, respectively (Ashby et al., 2007). The effective strain ( $e_{\text{eff}}$ ) is obtained as follows

$$e_{\text{eff}} = \sqrt{\frac{2}{3} \left[ e_{11}^2 + e_{22}^2 + e_{33}^2 + 2(e_{12}^2 + e_{23}^2 + e_{31}^2) \right]} \quad (8)$$

where  $e_{ij}$  ( $i, j = 1, 2, 3$ ) are Cartesian components of the Green-St. Venant strain tensor. The effective (von Mises) stress ( $\sigma_{\text{eff}}$ ) is calculated as

$$\sigma_{\text{eff}} = \sqrt{\frac{1}{2} \left[ (\sigma_{11} - \sigma_{22})^2 + (\sigma_{22} - \sigma_{33})^2 + (\sigma_{33} - \sigma_{11})^2 + 6(\sigma_{12}^2 + \sigma_{23}^2 + \sigma_{31}^2) \right]} \quad (9)$$

where  $\sigma_{ij}$  ( $i, j = 1, 2, 3$ ) are Cartesian components of the Cauchy stress tensor, respectively.

### 3. Results and discussion

We obtain that the largest displacements occur near the top medial bladder (Fig. 6a,b), mainly due to deformation caused by inflation of the bladder. The sock is much more strained than the strap and the maximal  $e_{\text{eff}}$  is near the top medial part of the brace (Fig. 6c,d). The stress, on the other hand, is primarily carried by the strap and the largest  $\sigma_{\text{eff}}$  is in the bladder regions (Fig. 7a,b). The difference in the  $e_{\text{eff}}$  and  $\sigma_{\text{eff}}$  distributions between the sock and the strap reflects the difference in their material properties. Since  $E_{\text{sock}} \ll E_{\text{strap}}$ , the sock easily deforms while the strap undergoes very little deformation. Consequently, the stresses generated in the sock are much smaller than the stresses generated in the strap. Importantly, calculated stresses are much smaller than the tensile strength limit of the proposed brace materials.

The largest pressures that the brace exerts on the knee occur in the strap region, including the areas where the bladders are located where the pressure is of a similar magnitude as the inflating pressure  $P$  (Fig. 7c,d). There are also two isolated "hot spots" located on the lateral side where the pressure exceeds the inflating pressure by nearly a factor of two (Fig. 7d). This is a concern since those high pressures regions may inflict discomfort and hamper local blood circulation. A possible measure that could reduce the pressure at the "hot spots" is to change elastic properties of the strap and the sock. For example, if the  $E_{\text{strap}}$  is reduced from  $5,000$  MPa to  $3,000$  MPa and the  $E_{\text{sock}}$  increases from  $1$  MPa to  $3$  MPa while keeping all other material and geometric parameters unaltered, the pressure at the hot spots is reduced by  $\sim 33\%$ .

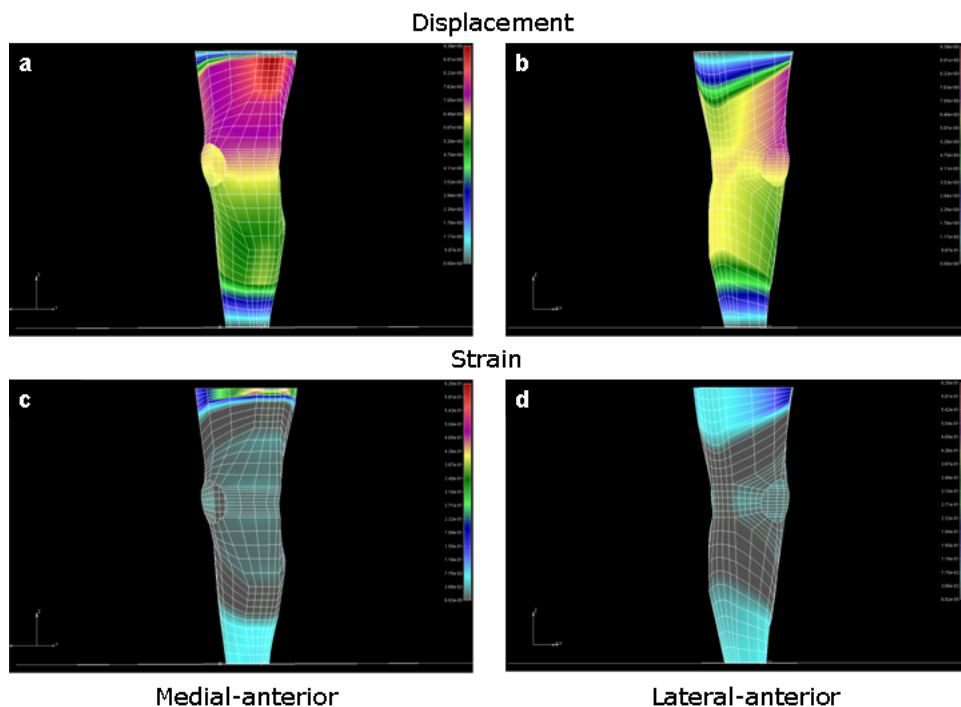


**Fig. 6.** Distributions of displacements (a, b) and of the effective strain (c,d) in response to bladder inflation to the pressure of 0.048 MPa. The maximal displacement of 0.94 cm is in the upper medial bladder region (a), whereas the maximal effective strain of 47% is near the top medial part of the brace (c). Results are obtained for the following parameter values:  $L_T = 20$  cm,  $L_B = 30$  cm,  $l_T = 10$  cm,  $l_B = 15$  cm,  $R_T = 16.5$  cm,  $R_B = 18.5$  cm, all bladders  $6 \times 6$  cm, hole diameter = 80 cm,  $E_{\text{strap}} = 3000$  MPa,  $\nu_{\text{strap}} = 0.3$ ,  $E_{\text{sock}} = 1$  MPa,  $\nu_{\text{sock}} = 0.43$  (for parameter identification see Fig. 3).

In general, the abduction moment  $M$  of the brace increases with increasing level of inflating bladder pressure  $P$ ;  $M$  vs.  $P$  curves generated for different combinations of geometrical and material parameter values are shown in Fig. 8. The most critical parameters appear to be the size of the medial bladders; for a given  $P$ , the greater the size of the bladder, the greater the  $M$ . Changes of other geometrical parameters and of the material properties of the brace components within the ranges given above have a smaller influence on  $M$  than the bladder size.

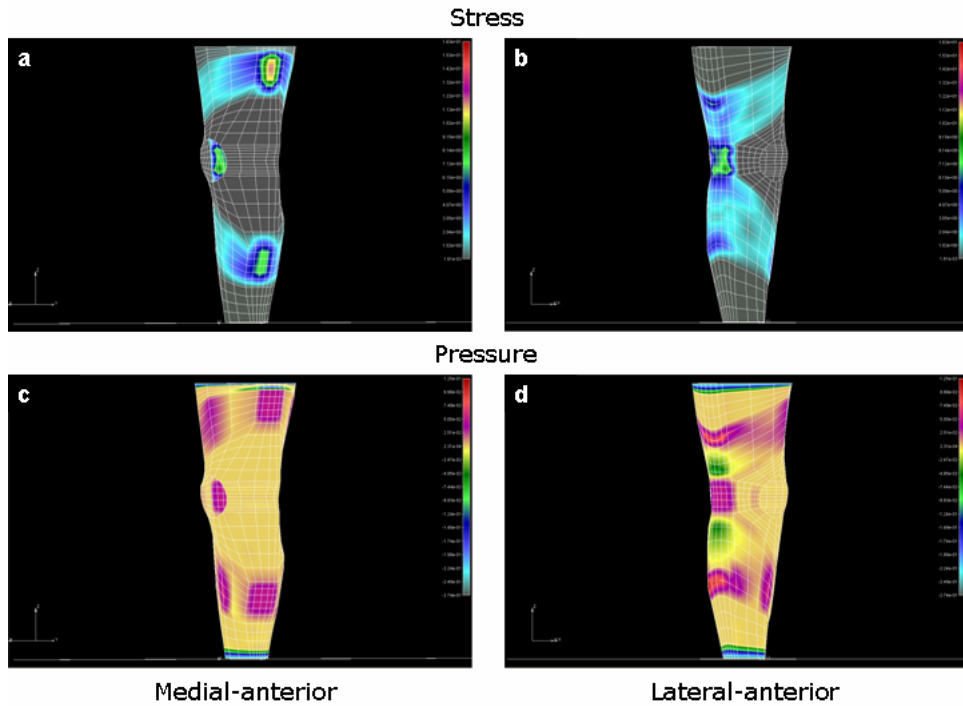


**Fig. 7.** Distributions of the effective (von Mises) stress (a, b) and of pressure exerted by the brace on the knee (c,d) in response to bladder inflation to the pressure of 0.048 MPa. The maximal effective stress of 11.2 MPa is in the upper medial bladder region (a), whereas the maximal pressure regions of 0.11 MPa are on the lateral side of the brace (d). Results are obtained for the following parameter values:  $L_T = 20$  cm,  $L_B = 30$  cm,  $l_T = 10$  cm,  $l_B = 15$  cm,  $R_T = 16.5$  cm,  $R_B = 18.5$  cm, all bladders  $6 \times 6$  cm, hole diameter = 80 cm,  $E_{\text{strap}} = 3000$  MPa,  $\nu_{\text{strap}} = 0.3$ ,  $E_{\text{sock}} = 1$  MPa,  $\nu_{\text{sock}} = 0.43$  (for parameter identification see Fig. 3).

To show that the brace can attenuate the excessive adduction moment  $\Delta M$ , we calculate  $\Delta M$  based on anatomical data for women and men from the literature and using Eq. (1). For  $\sim 45$  old women (average  $W = 72.4$  kg,  $h = 164.1$  cm),  $\Delta M = 11.65$  N·m and for  $\sim 45$  old men (average  $W = 84.6$  kg,  $h = 176$  cm),  $\Delta M = 14.61$  N·m. By normalizing  $M$  calculated from the finite-element model (see Fig. 8) with these values of  $\Delta M$ , we find that the brace is capable of completely attenuating  $\Delta M$  in women and  $\sim 90\%$  of  $\Delta M$  in men when the bladders are pressurized from 43 to 48 kPa. This is the most significant result of this study. It shows that in theory the pneumatic brace can unload a much greater fraction of the excessive adduction moment than what has been obtained from clinical testing of the existing rigid frame braces (10-13%) (Lindenfeld et al., 1997; Pollo et al., 2002). Despite these favorable theoretical results, it should be taken into consideration that the modeling of the brace includes several crude approximations and assumptions that are addressed below.

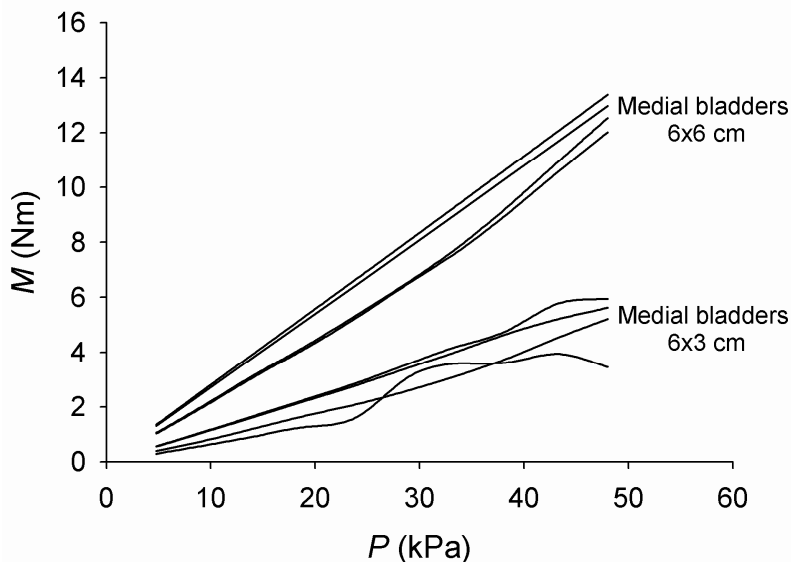


**Fig. 8.** Unloading abduction moment ( $M$ ) vs. bladder pressure ( $P$ ) relationships predicted by the finite element model for different sets of parameter values. The higher values of  $M$  are obtained with the 6×6 cm medial bladders than with 6×3 cm medial bladders. Variations of other geometrical and material parameters of the brace model have smaller effects on  $M$ .

We assume that the top and the bottom of the brace do not move relative to the leg. In reality, brace migration is common and patients must repeatedly reposition the brace throughout the day. For example, it is likely that the stress in the strap would tend to bring the medial bladders closer to each other, causing sliding of the brace relative to the leg and effectively shortening the brace. This, in turn would reduce the moment arm and thereby  $M$  would decrease. One measure to offset this effect is to insert flexible bars along the medial part of the brace to keep the medial bladders equidistant. Another measure is to increase the contact forces at the top and the bottom of the brace by additional straps around the leg.

We also assume that during inflation the contact area between bladders and the leg remains unaltered. In reality, this is not the case since during inflation the bladders tend to round up which would cause the contact area to decrease. Thus, the inflating pressure would be transmitted over a smaller area, which would mean a smaller net force exerted by the three point leverage on the knee and thereby a smaller  $M$ .

Another assumption is that the leg surface is regarded as a rigid body. However, the tissue around the knee is deformable, which would affect stress and strain distribution in the brace as well as  $M$ . For example, during inflation bulging bladders will push into compliant leg tissue thereby increasing the contact area between the bladders and the leg surface. This would cause an increase in force that the three-point leverage system exerts on the knee and thereby an increase in  $M$ .

The finite-element analysis considers only the case of static loading in a fully extended knee. However, during gait the knee undergoes dynamic loading and flexing which would certainly alter the distributions of  $e_{\text{eff}}$ ,  $\sigma_{\text{eff}}$ , and pressure on the knee, as well as  $M$ . Including these dynamic effects in the model would make the finite-element analysis much more complex and laborious. In this case, we believe that experimental studies on a prototype of a pneumatic

knee brace would be a more appropriate approach to analyzing brace's performance during gait. Nevertheless, the finite element analysis presented here is a valuable first step that provides results which have served as guidelines for the final design, manufacturing and clinical testing of the brace.

In summary, our finite element analysis has demonstrated the feasibility of developing a light, pneumatic knee brace, made of soft materials, which could effectively replace the existing bulky rigid-frame knee braces. The analysis shows that with moderate inflating pressures, the pneumatic knee brace can produce an unloading abduction moment that is capable of attenuating the negative effect of the adduction moment in a fully extended varus knee.

#### 4. Acknowledgement

This study is supported by a grant from Coulter Foundation, and grants No. OI-144028 and TR12007 from the Ministry of Science of Serbia.

#### 5. References

- (1998). Prevalence and impact of chronic joint symptoms--seven states, 1996, *MMWR - Morbidity & Mortality Weekly Report*, 47, 345-351.
- Ashby M, Shercliff H, Cebon D (2007). *Materials – Engineering, Science, Processing and Design*, Butterworth-Heinemann, UK.
- Felson DT, Lawrence RC, Hochberg MC, McAlindon T, Dieppe PA, Minor MA, Blair SN, Berman BM, Fries JF, Weinberger M, Lorig KR, Jacobs JJ, Goldberg V (2000). Osteoarthritis: new insights. Part 2: treatment approaches. *Ann. Intern. Med.* 133, 726-737.
- Giori N (2004). Load-shifting brace treatment for osteoarthritis of the knee: A minimum 2 1/2-year follow-up study. *J. Rehabil. Res. Dev.* 41, 187-194.
- Hurwitz DE, Ryals AB, Case JP, Block JA, Andriacchi TP (2002). The knee adduction moment during gait in subjects with knee osteoarthritis is more is more closely correlated with static alignment than radiographic disease severity, toe out angle and pain. *J. Orthop. Res.* 20, 101-107.
- Jones R (2002). Efficacy and safety of COX 2 inhibitors. *BMJ*, 325, 607-608.
- Juni P, Rutjes AWS, Dieppe PA (2002). Are selective COX-2 inhibitors superior to traditional non-steroidal anti-inflammatory drugs? *BMJ*, 324, 1287-1288.
- Kirkley A, Webster-Bogaert S, Litchfield R, Amendola A, MacDonald S, McCalden R, Fowler P (1999). The effect of bracing on varus gonarthrosis. *J. Bone Joint Surg.* 81, 539-548.
- Kojić M, Filipović N, Stojanović B, Kojić N (2008). *Computer Modeling in Bioengineering – Theoretical Background, Examples and Software*, J. Wiley and Sons, Chichester, UK.
- Kojić M, Slavković R, Živković M, Grujović N (1998). *PAK – Finite Element Program for Linear and Non-linear Structural Analysis, Mass and Heat Transfer and Biomechanics*, Faculty of Mechanical Engineering, University of Kragujevac, Kragujevac, Serbia.
- Komistek RD, Dennis DA, Northcut EJ, Wood A, Parker AW, Traina SM (1999). An in vivo analysis of the effectiveness of the osteoarthritic knee brace during heel-strike of gait. *J. Arthroplasty*, 14, 738-742.
- Lawrence RC, Helmick CG, Arnett FC, Deyo RA, Felson DT, Giannini EH, Heyse SP, Hirsch R, Hochberg MC, Hunder GG, Liang MH, Pillemer SR, Steen VD, Wolfe F (1998). Estimates of the prevalence of arthritis and selected musculoskeletal disorders in the United States. *Arthritis Rheum.* 41, 778-799.

- Lindenfeld TN, Hewett TE, Andriacchi TP (1997). Joint loading with valgus bracing in patients with varus gonarthrosis. *Clin. Orthop. Related Res.* 344, 290-297.
- Pollo F, Otis JC, Backus SI, Warren RF, Wickiewicz TL (2002). Reduction of medial compartment loads with valgus bracing of the osteoarthritic knee. *Am. J. Sports Med.* 30, 414-421.
- Schipplein OD, Andriacchi TP (1991). Interaction between active and passive knee stabilizers during level walking. *J. Orthop. Res.* 9, 113-119.
- Sharma L, Song J, Felson DT, Cahue S, Shamiyeh E, Dunlop DD (2001). The role of knee alignment in disease progression and functional decline in knee osteoarthritis. *JAMA*, 286, 188-195.
- Todd PA, Clissold SP (1990). Naproxen. A reappraisal of its pharmacology, and therapeutic use in rheumatic diseases and pain states. *Drugs*, 40, 91-137.
- Zhang W, Moskovitz R, Nuki G, Abramson S, Altman R, Arden N, Bierma-Zeinstra S, Brandt KD, Croft P, Doherty M, Dougados M, Hochberg M, Hunter DJ, Kwoh K, Lohmander LS, Tugwell P (2008). OARSI recommendations for the management of hip and knee osteoarthritis, Part II: OARSI evidence-based, expert consensus guidelines. *Osteoarthr. Cartilage*, 16, 137-162.